Cellular Signalling 63 (2019) 109378

Contents lists available at ScienceDirect

Cellular Signalling

journal homepage: www.elsevier.com/locate/cellsig

Deletion of HO-1 blocks development of B lymphocytes in mice

Zhen Zhou[a,b,e,1], Dan Ma[a,c,d,1], Ping Liu[a,c,d], Ping Wang[a,c,d], Danna Wei[a,c,d], Kunling Yu[a,c,d], Peifan Li[f], Qin Fang[b,e], Jishi Wang[a,c,d,*]

[a] Department of Hematology, Affiliated Hospital of Guizhou Medical University, Guiyang 550004, China
[b] Department of Pharmacy, Affiliated Baiyun Hospital of Guizhou Medical University, Guiyang 550004, China
[c] Key Laboratory of Hematological Disease Diagnostic and Treat Centre of Guizhou Province, Guiyang 550004, China
[d] Department of Hematology, Guizhou Provincial Laboratory of Hematopoietic Stem Cell Transplantation Center, Guiyang 550004, China
[e] Department of Pharmacy, Affiliated Hospital of Guizhou Medical University, Guiyang 550004, China
[f] Department of Psychiatry, Affiliated Hospital of Guizhou Medical University, Guiyang 550004, China

ARTICLE INFO

Keywords:
Gene knockout
Heme oxygenase-1
B lymphocyte
Development
Mice

ABSTRACT

B lymphocytes, a key cluster of cells composing the immune system, can protect against abnormal biological factors. Heme oxygenase-1 (HO-1) plays important roles in cell proliferation and immune regulation, but its effects on the development and growth of B lymphocytes are still unknown. Herein, the count of B lymphocytes in HO-1 gene knockout (HO-$1^{+/-}$) mice was significantly lower than that of the HO-1 gene wild-type (HO-1^{WT}) mice. Meanwhile, the cell count of HO-$1^{+/-}$ mice did not recover after irradiation for one week, due to the G0/G1 phase arrest of Pro-B cells and the augmented apoptosis of Pre-B cells. Up-regulation of HO-1 by lentivirus attenuated the Pro-B cell cycle arrest and Pre-B cell apoptosis. To understand the molecular mechanism by which HO-1 knockout blocked B lymphocyte development, protein-to-protein interaction network and Western blot were used. The PI3K/AKT signaling pathway mediated the regulatory effects of HO-1 on B lymphocytes. In conclusion, HO-1 is a crucial transcriptional repressor for B cell development.

1. Introduction

The hematopoietic system is a distributed tissue consisting of multiple phenotypically and functionally distinct cell types [1,2]. B cells are essential for the hematopoietic system, functioning as efficient immune responses to a variety of pathogens [3]. B cells develop from hematopoietic precursor cells in an ordered maturation and selection process. Defects in B cell development, selection and function lead to autoimmune disease, malignancy, immunodeficiency and allergy [4]. Therefore, clarifying the key regulators of B cell differentiation and immune function is of great significance to the treatment of related diseases.

Heme oxygenase-1 (HO-1) is a heme catabolic enzyme responsible for the degradation of hemoglobin into carbon monoxide, bilirubin and biliverdin [5,6]. Besides, it is capable of protecting cells, resisting apoptosis, promoting proliferation and regulating cellular immunity [7]. For hematopoietic system diseases, overexpression HO-1 enhances the anti-apoptotic and cell cycle-blocking effects of leukocytes, causing resistance to chemotherapeutic drugs [8,9]. In addition, the influence of HO-1 on cell differentiation in microenvironment has attracted widespread attention. We have previously reported that overexpression of HO-1 in bone marrow stromal cells enhanced microenvironment-mediated anti-apoptotic effects [10]. Similarly, Herroon et al. demonstrated that up-regulation of HO-1 promoted cell survival in bone marrow via oxidative and endoplasmic stress pathways [11]. HO-1 influences a lineage commitment in pluripotent stem cells and maturation of hematopoietic cells [12,13], so it may play an important role in microenvironment. However, whether HO-1 can promote B cell differentiation and development, especially in the bone marrow microenvironment, remains elusive.

To explore the role of HO-1 in microenvironment, HO-1 gene knockout mice were established. Meanwhile, mice with homozygous deletion of HO-1 gene (HO-$1^{-/-}$ mice) were also established. However, the number of HO-$1^{-/-}$ mice was significantly lower than the Mendelian expectation ratio (about 2%) [14–16]. Indeed, HO-1 heterozygous (HO-$1^{+/-}$) mice were not perfect subjects, but we had to use them in subsequent experiments to ensure the study feasibility. Similarly, HO-$1^{+/-}$ mice have been utilized in a previous literature [17].

* Corresponding author at: Guizhou Province Laboratory of Hematological Disease Diagnostic & Treat Centre, Department of Hematology, Affiliated Hospital of Guizhou Medical University, Guizhou Province Hematopoietic Stem Cell Transplantation Centre, Guiyang, Guizhou 550004, China.
E-mail address: wangjijshi9646@163.com (J. Wang).
[1] Co-First author, Dan Ma and Zhen Zhou contribute equally to this study.

https://doi.org/10.1016/j.cellsig.2019.109378
Received 27 March 2019; Received in revised form 25 July 2019; Accepted 27 July 2019
Available online 29 July 2019
0898-6568/

Interestingly, the count of $CD19^+$ B cells in the peripheral blood (PB) of HO-$1^{+/-}$ mice was significantly lower than that of HO-1 gene wild-type (HO-1^{WT}) mice. Additionally, the absolute numbers of $CD45^+$/$CD19^+$ cells in the PB and spleen of HO-$1^{+/-}$ mice were lower than those of HO-1^{WT} mice, and the spleen and bone marrow of HO-$1^{+/-}$ mice also had significantly fewer B cell subsets. Moreover, the count of irradiated $CD45^+$/$CD19^+$ cells from HO-1^{WT} mice returned to normal after a week, whereas that of HO-$1^{+/-}$ mice remained low. Therefore, we hypothesized that HO-1 knockout evidently affected the differentiation of B cells in bone marrow.

Herein, we studied the development of B cells in HO-1 knockout mice, aiming to elucidate the effects of HO-1 on B cell development and to provide a new target for treating related diseases.

2. Methods

2.1. Mice

HO-1 knockout mice described in Supplementary Material were provided by Cyagen Biosciences Inc. (USA). Experiments were performed with 4- to 6-week-old mice. All procedures involving mice were approved by the Ethics Committee of Affiliated Hospital of Guizhou Medical University, and conducted in accordance with Guidelines for the Care and Use of Laboratory Animals [18]. Immunodeficient mice were established by being placed into an acrylic circular container and exposed to 4.5 Gy X-ray at a dose rate of 1.2 Gy/min (RS2000Pro, Rad Source Technologies, USA) [19–21]. All mice were housed under specific pathogen-free conditions.

2.2. Flow cytometry (FCM) and fluorescence-activated cell sorting (FACS)

Cells were extracted from bone marrow and spleen, passed through a 200-mesh sieve for subsequent FCM and FACS, and stained with anti-B220 (PerCP-Cy5.5), anti-CD43 (APC), anti-IgM (FITC), anti-IgD (PE), anti-CD21 (FITC), anti-CD23 (PE), anti-CD25 (APC) and anti-CD93 (APC) for 30 min at 4 °C in dark. Then the stained cells were analyzed by FCM on LSR II (BD Biosciences, USA), and FACS was performed on FACS Aria II (BD Biosciences, USA) [22]. For FACS, the cells were concentrated to 10 million ml^{-1} by resuspension in phosphate buffered saline (PBS) after staining to maintain a sorting rate of about 1000 cells/s [23,24].

The parameters for FCM visualization of B lineage populations were as follows: Immature B cells (IM, flow phenotype: B220 + IgM+), mature recirculating B cells (MR, flow phenotype: B220 + IgM + IgD+), mature B cells (M, flow phenotype: B220 + IgM + IgD+) marginal zone cells (MZ cells, flow phenotype: CD21brightCD23+), follicular cells (FO cells, flow phenotype: CD21 + CD23brightCD93-) and transitional B cells (Tra cells, flow phenotype: CD21 + CD23brightCD93+).

2.3. Cells and culture conditions

B cell precursor (Pre-B, flow phenotype: $B220^+CD43^+IgM^-$) and B cell progenitor (Pro-B, flow phenotype: $B220^+CD43^-IgM^-$) cells were sorted by using the bone marrow from HO-1^{WT} and HO-$1^{+/-}$ mice. Subsequently, all cells were maintained in StemPro®-34 SFM complete medium (No. 10639011, Thermo Fisher Scientific, USA) supplemented with 50% B liquid nutrient supplement (No. A1024001, Thermo Fisher Scientific, USA). The cells were maintained in a 37 °C incubator with 95% humidity and 5% CO_2 [25–28].

2.4. Real-time PCR

Total RNA was extracted from cells using TRIzol reagent (Invitrogen, USA), and cDNA was synthesized using Prime Script reverse transcription kit (Takara, China). Real-time PCR was conducted on iQ5 Multicolor real-time PCR system (Bio-Rad Laboratories Inc., USA) using SYBR Green Real-time PCR Master Mix (Takara, China). Amplification was carried out under the following conditions: denaturation at 94 °C for 3 min, 35 cycles of 94 °C for 30 s, 58 °C for 30 s and 72 °C for 35 s. The expression of target gene was calculated using the $2^{-\Delta\Delta Cq}$ method [29–31]. All experiments were repeated independently 3 times.

2.5. Lentiviral vector transduction

Sequences containing mouse coding sequence of HO-1 gene were selected with Invitrogen designer software. Retroviruses were generated by transfecting empty plasmid vector containing HO-1 plus enhanced green fluorescence protein (EGFP) into 293 T packaging cells, using FuGENE HD6. Lentiviral stocks were concentrated using Lenti-X concentrator, and titers were determined with Lenti-X Q-PCR titration kit (Shanghai Innovation Biotechnology Co., Ltd., China). Finally, four recombinant lentiviral vectors were constructed: lentivirus-V5-D-TOPO-HO-1-EGFP (L-HO-1) and lentivirus-V5-D-TOPO-EGFP (TOPO-EGFP). For transduction, the cells were inoculated into 12-well plates at 2.5×10^5/well, infected with the lentiviral stocks at a multiplicity of infection of 10 in the presence of polybrene (10 μg/ml), and then analyzed by Olympus fluorescence microscope (Japan) and Western blotting 48 h after transduction. MEC-1 cells were transduced with L-HO-1 (HO-1) and TOPO-EGFP (Vector), respectively [32,33].

2.6. Pathological and hematoxylin-eosin (HE) staining

Splenic tissues were fixed in neutral formalin for one day. Bone marrow tissues were fixed in neutral formalin for one week and decalcified for one day. The splenic and bone marrow tissues were embedded in paraffin blocks, sectioned and stained with HE [18].

2.7. Apoptosis analysis

Cells were treated with lentivirus for 72 h, harvested, washed with PBS and stained with 7AAD according to the manufacturer's instructions. They were thereafter subjected to FCM using Cell Quest software (BD Biosciences, USA) [2,34].

2.8. Cell viability

Cell viability was measured using trypan blue (Solarbio, China) after trypan staining [35]. The stained cells were observed under Nikon microscope (Japan).

2.9. Cell cycle analysis

Cell cycle was measured using FCM system (BD Biosciences, USA) after propidium iodide staining. The DNA content was detected by FCM, and cell cycle distributions were analyzed with Cell Quest Pro software (BD Biosciences, USA) [32,33].

2.10. Western blot

Protein expressions were detected by Western blot. Primary antibodies against HO-1, AKT and P-AKT were obtained from Santa Cruz Biotechnology (USA). P was used to represent phosphorylation. Cell cycle-related antibodies against P21, P27, CDK4 and CDK6 as well as secondary antibodies were purchased from Cell Signaling Technology (USA). Apoptosis-related antibodies against BAD and BCL-2 were bought from Abcam (USA). Equal amounts of protein lysate were used for Western blot analyses [10,32,36,37], and β-actin expressions were maintained consistent.

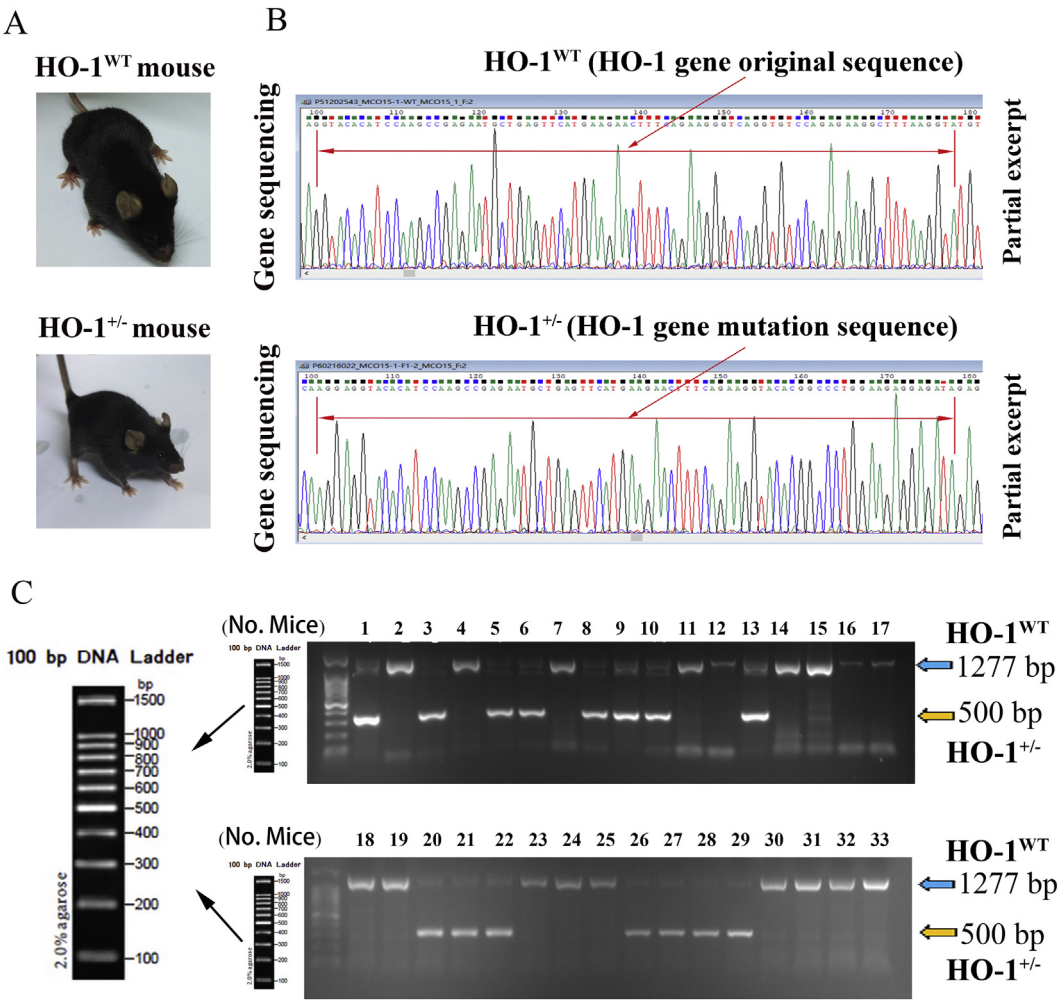

Fig. 1. Characteristic descriptions and identification of HO-1^{WT} and HO-$1^{+/-}$ mice.
(A) HO-1 gene was knocked out using CRISPR/Cas technology. HO-1 knockout mice were housed under specific pathogen-free conditions, and the survival statuses of HO-1^{WT} and HO-$1^{+/-}$ mice were observed every day. (B) Sanger sequencing confirmed HO-1 gene sequences. (C) The first-generation HO-$1^{+/-}$ mice were bred, giving more mice with different HO-1 genotypes, which were then identified as HO-$1^{+/-}$ (500 bp) or HO-1^{WT} (1277 bp) by PCR., HO-1^{WT} mice stands for the HO-1 gene wild type mice and HO-$1^{+/-}$ mice stands for the HO-1 gene heterozygous mice.

3. Results

3.1. Establishment of HO-1 gene knockout mice and detection of HO-1 gene expression

We knocked out HO-1 gene from C57/BL6 mice using CRISPR/Cas technology. HO-1 gene knockout mice have previously been established with this method [16]. Actually, we have also established mice with homozygous deletion of HO-1 gene (HO-$1^{-/-}$ mice). However, the number of HO-$1^{-/-}$ mice was too small (Mendelian expectation ratio of about 2%), failing to meet the experimental requirements. To ensure the study feasibility, we used HO-$1^{+/-}$ mice in subsequent experiments. Notably, the HO-$1^{+/-}$ mouse was smaller than the HO-1^{WT} mouse, with their survival statuses shown in Fig. 1A. To verify that the establishment was successful, the HO-1 gene sequences of HO-1^{WT} and HO-$1^{+/-}$ mice were detected by DNA sequencing (Fig. 1B). In panel B, the upper part exhibits the nucleotide sequence of HO-1^{WT} mouse, and the lower part shows a mismatched nucleotide sequence, indicating that HO-1 gene had been knocked out. Next, the first-generation HO-$1^{+/-}$ mice were bred. Since the cost of sequencing was high, HO-$1^{+/-}$ mice were identified by PCR by extracting mouse tissue DNA. PCR showed that HO-$1^{+/-}$ and HO-1^{WT} mice had different HO-1 DNA molecular weights, because HO-1 gene in HO-$1^{+/-}$ mouse had only half of alleles. Therefore, the band of HO-1 gene appears at near 500 bp, and that of HO-1^{WT} mouse is located at approximately 1277 bp. As a result, HO-$1^{+/-}$ mice can be identified. The mice numbered 1, 3, 5, 6, 8, 9, 10, 13, 20, 21, 22, 26, 27 and 28 were HO-1^{WT} mice, and those numbered 2, 4, 7, 11, 12, 14, 15, 16, 17, 18, 19, 23, 24 and 25 were HO-$1^{+/-}$ mice (Fig. 1C).

3.2. Expressions of HO-1 gene and protein in HO-$1^{+/-}$ mice were significantly lower than those in HO-1^{WT} mice

Real-time PCR and Western blot showed that the expressions of HO-1 gene and protein in HO-$1^{+/-}$ mice were significantly lower than those of HO-1^{WT} mice ($P < 0.05$, $P < 0.01$) (Fig. 2A-C). Notably, the HO-1 gene and protein expressions of HO-$1^{+/-}$ mice were significantly lower than those of HO-1^{WT} mice. Therefore, HO-$1^{+/-}$ mice were used. For subsequent experiments, we selected the HO-$1^{+/-}$ mice with significantly lower HO-1 gene and protein expressions.

3.3. B cells in bone marrow and spleen of HO-$1^{+/-}$ mice significantly reduced

We prepared immunodeficient mice through irradiation (dose: 4.5 Gy/mouse) to establish a hematological tumor model by injecting

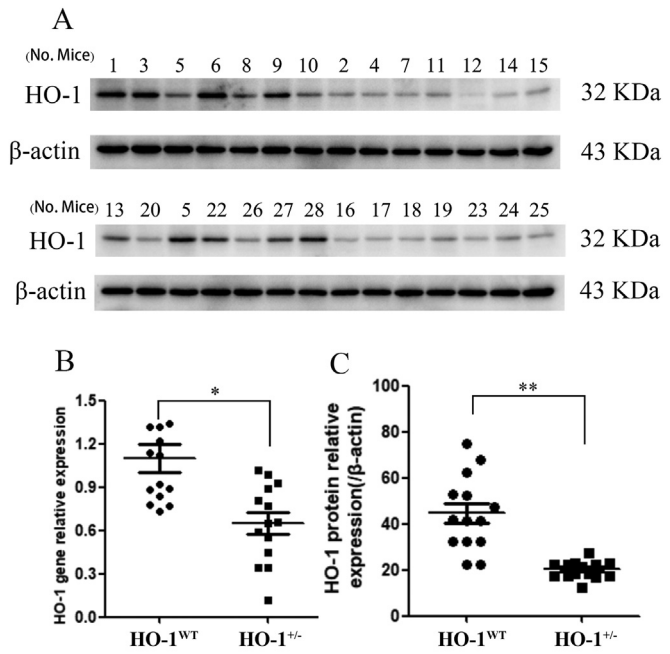

Fig. 2. HO-1 protein expressions in HO-1^{WT} and HO-1$^{+/-}$ mice.
(A and B) The expressions of HO-1 gene and protein in HO-1^{WT} and HO-1$^{+/-}$ mice were detected by Western blot and real-time PCR, respectively. Western blot bands were quantified with Quantity One software. Data were analyzed with GraphPad Prism V5.0 software (San Diego, CA, USA). All experiments were repeated three times. *P < 0.05, **P < 0.01.

human leukocytes. To assess the damage of the immune system after irradiation, CD19$^+$ cells in PB of mice were counted on day 0 and day 7, respectively. The number of CD19$^+$ B cells in PB of HO-1$^{+/-}$ mice was significantly lower than that of HO-1^{WT} mice on day 0 (P < 0.05) (Fig. 3A). On day 7, the count of CD19$^+$ B cells in PB of HO-1^{WT} mice returned to normal, but that of HO-1$^{+/-}$ mice failed to do so (compared with day 0, P < 0.05) (Fig. 3B). Furthermore, FCM exhibited that HO-1^{WT} and HO-1$^{+/-}$ mice had similar numbers of CD3$^+$ T cells (P > 0.05) (Supplementary Fig. 1), but there were significantly different counts of CD19$^+$ B cells. Based on the above findings, we further extracted mouse bone marrow and spleen, and detected CD45$^+$CD19$^+$ B cells therein by absolute counting with FCM. The counts of CD45$^+$CD19$^+$ B cells in the PB and bone marrow HO-1$^{+/-}$ mice were significantly lower than those of HO-1^{WT} mice (P < 0.05) (Fig. 4A, Fig. 4B and Supplementary Fig. 2). Afterwards, the effects of HO-1 deficiency on later B cell developmental stages were assessed. Compared with littermate controls, HO-1$^{+/-}$ mice had significantly larger spleens and heavier weights (P < 0.05) (Fig. 4C). HE staining showed significantly fewer germinal centers in HO-1$^{+/-}$ mice than in HO-1^{WT} mice, which may be one of the causes for the decrease of B cells in PB. Next, we studied B cell maturation in the spleen of HO-1$^{+/-}$ mice and their littermate control HO-1^{WT}.

In particular, HO-1 deficient mice had significantly fewer immature, marginal zone, follicular and transitional B cells (P < 0.01, P < 0.05, P < 0.01 and P < 0.05) (Fig. 4E and Supplementary Fig. 3). In addition, FCM of various B cell subsets in bone marrow showed that HO-1 deficiency caused Pro-B cells to undergo a series of differentiation steps during the abnormal generation of Pre-B cells, and then blocked B cell development (P < 0.01) (Fig. 4F and Supplementary Fig. 4). The number of Pre-B cells was significantly smaller while immature and mature recirculating B cells were hardly detectable in the bone marrow of HO-1$^{+/-}$ mice (P < 0.01 and P < 0.05).

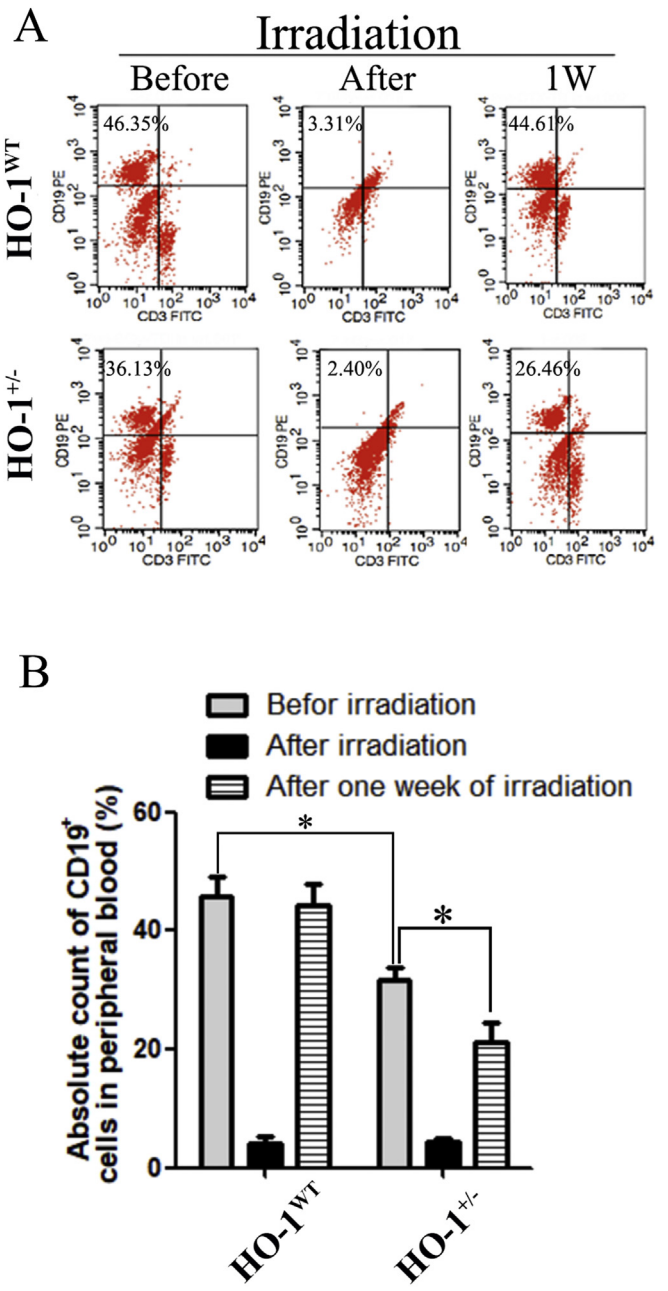

Fig. 3. Effect of irradiation on B cell growth in HO-1^{WT} and HO-1$^{+/-}$ mice.
(A) CD19$^+$ B cells in PB of HO-1$^{+/-}$ and HO-1^{WT} mice before and after irradiation were counted by FCM. (B) Absolute numbers of CD19$^+$ B cells in PB of HO-1$^{+/-}$ and HO-1^{WT} mice (n = 10).

3.4. B cell cycle arrest and apoptosis in HO-1$^{+/-}$ mice were significantly facilitated compared with those in HO-1^{WT} mice

The blockage of B lymphocyte development may mainly be attributed to cell cycle arrest and apoptosis, so we detected the two processes in the Pro-B and Pre-B cells of HO-1$^{+/-}$ mice and HO-1^{WT} mice by FCM. The Pro-B cell cycle of the HO-1$^{+/-}$ group was significantly arrested in the G1 phase (P < 0.01), but hardly altered in any pre-B cells subset in the absence of HO-1 (Fig. 5A). Additionally, the apoptosis rate of Pre-B cells in the HO-1$^{+/-}$ group exceeded that of the HO-1^{WT} group (P < 0.01), whereas the rates of Pro-B cells were similar (Fig. 5B). Collectively, HO-1 was essential for normal B lymphocyte development and its absence was associated with severe lymphopenia.

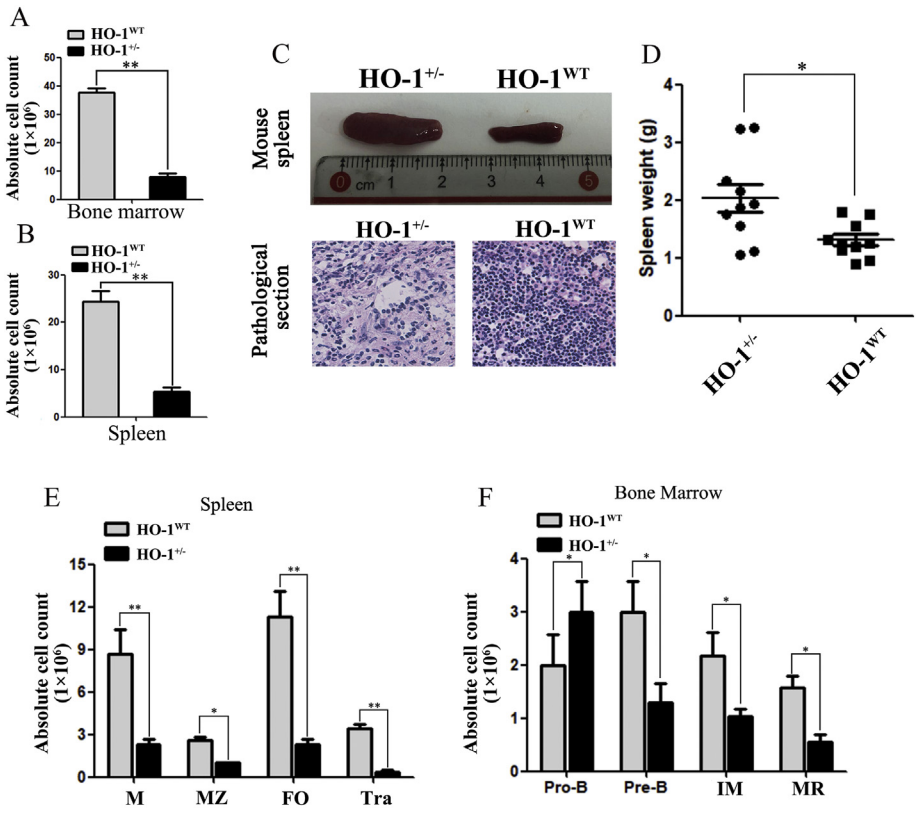

Fig. 4. HO-1 was required for early B cell development.
(A and B) Absolute numbers of $CD45^+CD19^+$ B cells in bone marrow and spleen of HO-$1^{+/-}$ and HO-1^{WT} mice (n = 10). (C) The spleen sizes of HO-$1^{+/-}$ and HO-1^{WT} mice were measured by calipers. Pathological changes were observed by HE staining. (D) The spleens of HO-$1^{+/-}$ and HO-1^{WT} mice were weighed by an electronic balance. (E) The spleen B cell subsets from HO-1^{WT} and HO-$1^{+/-}$ mice were detected by FCM (n = 10): absolute numbers of $B220^+IgM^+IgD^+$ mature (M), $CD21brightCD23^+$ marginal zone (MZ), $CD21^+CD23brightCD93^-$ follicular (FO) and $CD21^+CD23brightCD93^+$ transitional (Tra) B cells. (F) The bone marrow B cell subsets from HO-1^{WT} and HO-$1^{+/-}$ mice were detected by FCM (n = 10): absolute numbers of $B220^+CD43^+IgM^-$ pro-B cells, $B220^+CD43^-IgM^-$ pre-B cells, $B220^+IgM^+$ immature (IM) B cells and $B220^+IgM^+IgD^+$ mature recirculating (MR) B cells.

3.5. Knockout of HO-1 gene induced Pro-B cell cycle arrest

To gain an insight into the mechanism underlying the influence of HO-1 gene on Pro-B cell cycle arrest, we used lentiviral transduction to down-regulate HO-1 gene in the Pro-B cells of HO-1^{WT} mice and to up-regulate it in the cells of HO-$1^{+/-}$ mice. EGFP was detected with fluorescence microscopy (Fig. 6A). HO-1 gene and protein expressions in the transfected Pro-B cells were detected by real-time PCR and Western blot, respectively. The expressions in the transfected Pro-B cells of HO-1^{WT} mice were both significantly lower than those of the Vector1 group ($P < 0.01$), and the expressions in the Pro-B cells of HO-$1^{+/-}$ mice were significantly higher than those of the Vector2 group ($P < 0.01$). Next, the cell cycle arrests of different groups of Pre-B cells were detected by FCM. Silencing HO-1 gene in the Pro-B cells of HO-1^{WT} mice significantly blocked them in the G1 phase ($p < 0.05$), whereas up-regulating this gene in the cells of HO-$1^{+/-}$ mice significantly attenuated the blockage ($P < 0.05$) (Fig. 6B). Taken together, HO-1 protein weakened the cell cycle arrest of Pro-B cells.

3.6. Knockout of HO-1 gene enhanced Pre-B cell apoptosis

To further assess the effects of HO-1 on Pre-B cell apoptosis, we performed lentiviral transduction to silence HO-1 gene in the Pre-B cells of HO-1^{WT} mice and to up-regulate it in the cells of HO-$1^{+/-}$ mice. EGFP was detected with fluorescence microscopy (Fig. 7A). The HO-1 gene and protein expressions in the Pre-B cells of HO-1^{WT} mice significantly decreased compared with those of the Vector1 group, and the expressions in the cells of HO-$1^{+/-}$ mice significantly increased compared with those of the Vector2 group. Compared with control and vector groups, the apoptosis rate of Pre-B cells in the HO-1 up-regulation group significantly decreased. On the contrary, silencing HO-1 elevated the apoptosis rate ($P < 0.05$) (Fig. 7B). In short, HO-1 protein inhibited Pre-B cell apoptosis.

3.7. The PI3K/AKT pathway was involved in the relationship between HO-1 and Pro-B cell cycle arrest

To explore the mechanism by which HO-1 weakened Pro-B cell cycle arrest, we tested the key pathway related to B cell differentiation, i.e. the PI3K/AKT pathway. The expressions of HO-1, P-AKT, AKT, P21, P27, CDK4 and CDK6 proteins were detected by Western blot.

The expression of HO-1 protein in the HO-1^{WT} group significantly exceeded that of the HO-$1^{+/-}$ group. Lentivirus-mediated HO-1 up-regulation significantly increased HO-1 gene expression in the HO-$1^{+/-}$ group. Furthermore, up-regulating HO-1 protein in the Pro-B cells of HO-$1^{+/-}$ mice increased the expression of P-AKT protein, thereby attenuating the inhibited expressions of downstream cycling proteins such as P21, P27, CDK4 and CDK6 ($P < 0.05$) (Fig. 8A and B). In contrast, lentivirus-mediated HO-1 down-regulation significantly decreased HO-1 gene expression in the HO-1^{WT} group, and silencing HO-1 protein in the Pre-B cells of HO-1^{WT} mice reduced the expression of P-AKT protein, thus reversing the suppressed expressions of P21, P27, CDK4 and CDK6.

3.8. The PI3K/AKT pathway was involved in the relationship between HO-1 and Pre-B cell apoptosis

To explore the mechanism by which HO-1 protected against Pre-B cell apoptosis, we tested the key pathway related to B cell differentiation, i.e. the PI3K/AKT pathway. The expressions of HO-1, P-AKT, AKT, BAD and BCL-2 proteins were detected by Western blot.

The expression of HO-1 protein in the HO-1^{WT} group significantly surpassed that of the HO-$1^{+/-}$ group. Lentivirus-mediated HO-1 up-regulation significantly increased HO-1 gene expression in the HO-$1^{+/-}$ group. Besides, up-regulating HO-1 protein in the Pre-B cells of HO-$1^{+/-}$ mice increased the expression of P-AKT protein, thereby suppressing the expression of downstream apoptosis protein BAD but stimulating that of BCL-2 protein (Fig. 9A and B). In contrast, lentivirus-mediated HO-1 down-regulation significantly reduced HO-1 gene

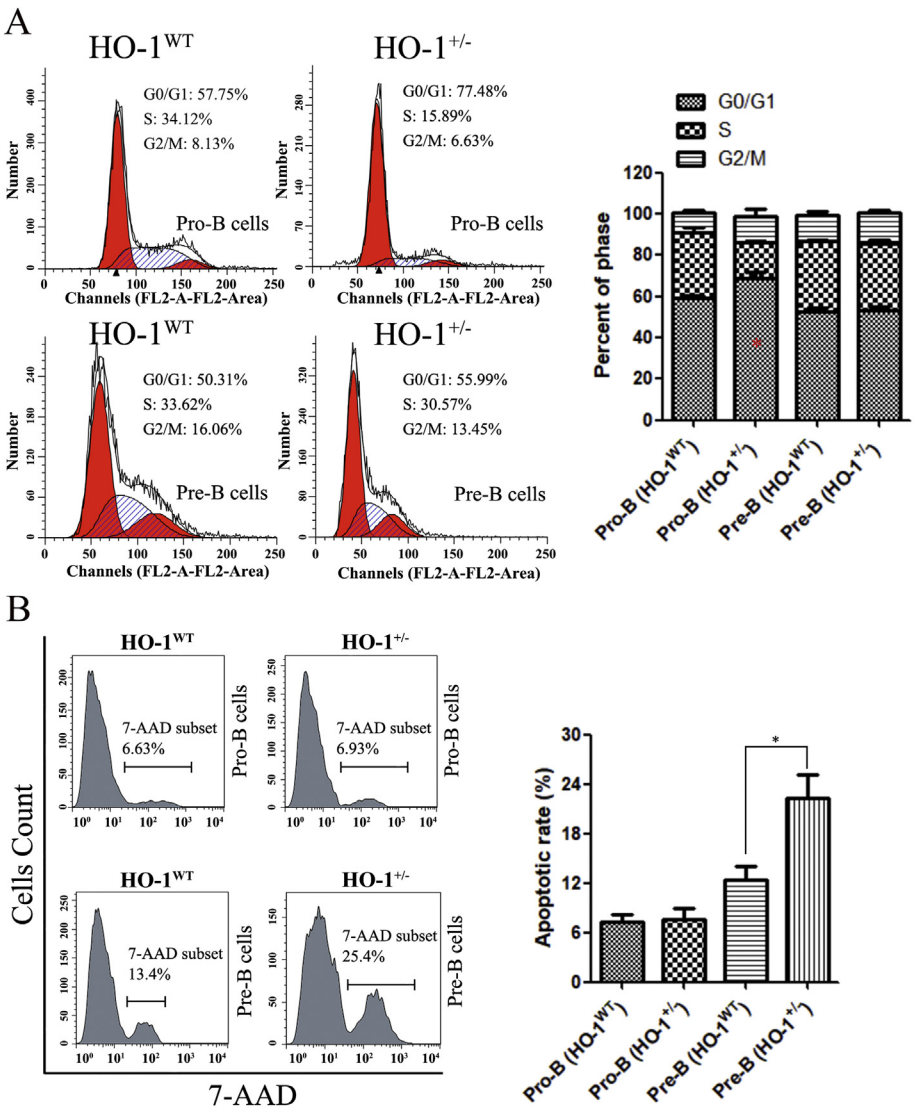

Fig. 5. Cell cycle and apoptosis changes of Pre-B and Pro-B cells.
(A and B) Pre-B and Pro-B cells were isolated from bone marrow cells of HO-1^{WT} and HO-$1^{+/-}$ mice by FACS. Next, cells apoptosis and cycle were detected by FCM. Data were analyzed with GraphPad Prism V5.0 software. All experiments were repeated three times. *P < 0.05, **P < 0.01.

expression in the HO-1^{WT} group, and silencing HO-1 protein in the Pre-B cells of HO-1^{WT} mice decreased the expression of P-AKT protein, reversing the above phenomenon.

3.9. Possible mechanism for influence of HO-1 on B cell development

HO-1 was required for AKT-mediated inhibition of apoptosis and cell cycle arrest, so we postulated that HO-1 was a key factor regulating the proliferation and development of B cells in mice. The mechanism for the relationship between HO-1 and the PI3K/AKT pathway is schematized in Fig. 10.

4. Discussion

At present, the roles of HO-1 in tumor microenvironment-mediated drug resistance, immune regulation, cytoprotection against inflammatory diseases and risk evaluation have been extensively studied on cellular and molecular levels [8,9,38–40]. Our group has devoted to studying the effects of HO-1 on hematological malignancies and the mechanisms, and demonstrated that HO-1 enabled acute myelocytic leukemia, chronic myelocytic leukemia, myelodysplastic syndrome, multiple myeloma and diffuse large B-cell lymphoma cells to resist various chemotherapeutic drugs [10,30–33,37,41–45]. Until now, however, the effects of HO-1 on B cell differentiation and the mechanisms are still unclear.

In this study, we used CRISPR/Cas9 technology to knock out HO-1 gene from mice, and obtained mice with different HO-1 genotypes. HO-1 was differently expressed in HO-1^{WT} and HO-$1^{+/-}$ groups, so we selected the mice with HO-1 expression differences for subsequent experiments. Then we prepared immunodeficient mice through irradiation and established a hematological tumor model by injecting human leukocytes [21]. The number of $CD19^+$ B cells in PB of HO-$1^{+/-}$ mice was significantly lower than that of HO-1^{WT} mice. Moreover, the recovery ability of B cells in PB of HO-$1^{+/-}$ mice was significantly inferior to that of HO-1^{WT} mice. Subsequently, FCM revealed that HO-1^{WT} and HO-$1^{+/-}$ mice had similar numbers of $CD3^+$ T cells. Nevertheless, the absolute numbers of $CD45^+CD19^+$ B cells in the bone marrow and spleen of HO-$1^{+/-}$ mice plummeted compared with those of littermate controls. Thus, HO-1 predominantly participated in B cell development.

Once generated, Pro-B cells undergo a series of differentiation steps that generate Pre-B cells and immature B lymphocytes. The latters then migrate to the spleen to complete their maturation. Hence, we firstly

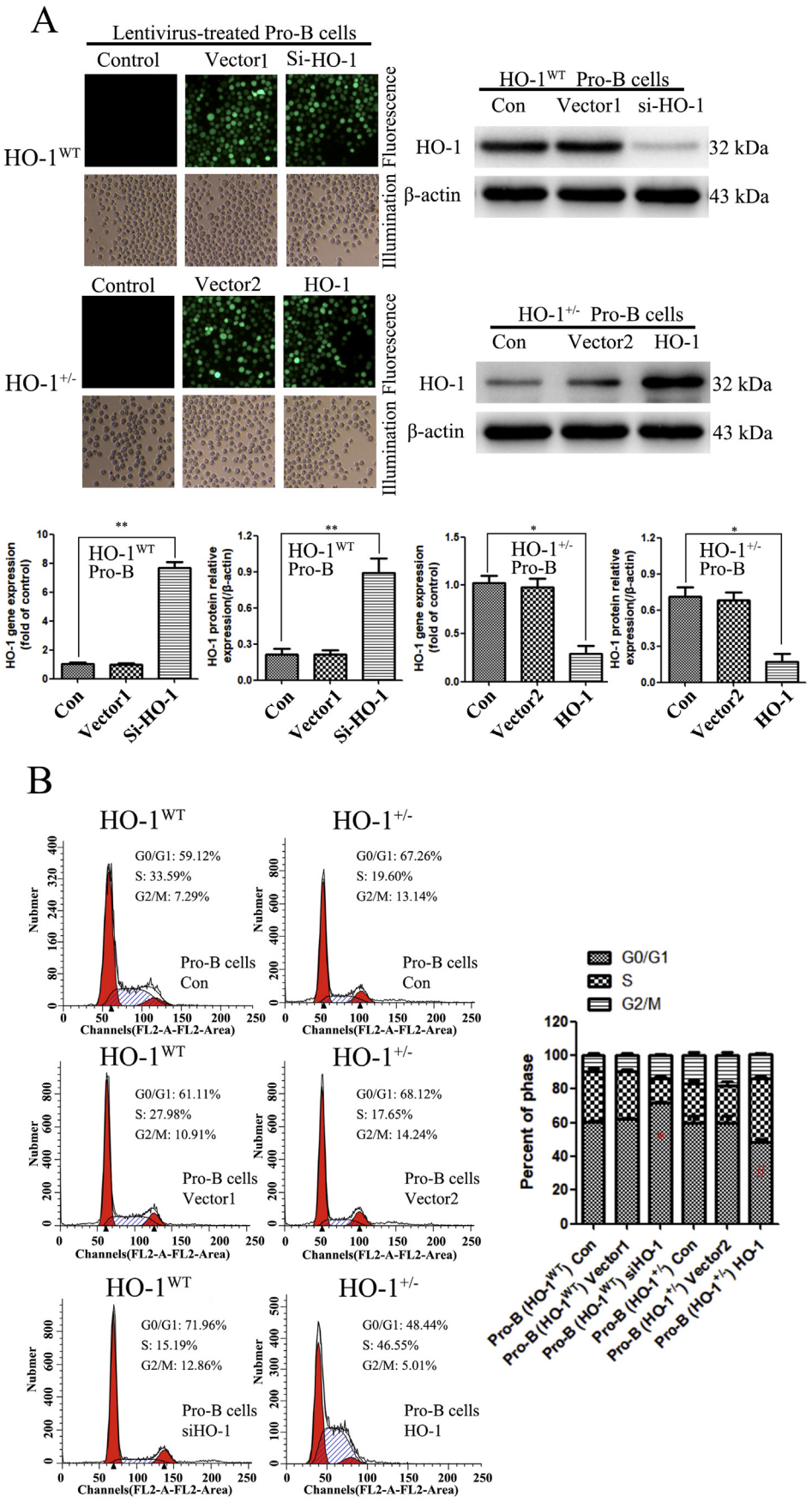

Fig. 6. Effects of HO-1 protein on Pro-B cell cycle arrest.

(A) Pro-B cells were isolated from bone marrow cells of HO-1^{WT} and HO-$1^{+/-}$ mice by FACS. Next, lentivirus-mediated HO-1 gene over-expression in Pro-B cells of HO-$1^{+/-}$ mice and HO-1 gene silencing in Pro-B cells of HO-1^{WT} mice, as well as positivity of lentivirus-mediated HO-1 transduction (> 95%) were observed by fluorescence microscopy. HO-1 gene and protein expressions were detected by real-time PCR and Western blot, respectively. (B) After treatment with lentivirus for 48 h, cells cycle arrest was detected by FCM. *Comparison between control and siHO-1 in HO-1^{WT} mice, $P < 0.05$. #Comparison between control and siHO-1 in HO-$1^{+/-}$ mice, $P < 0.01$. Data were analyzed with GraphPad Prism V5.0 software.

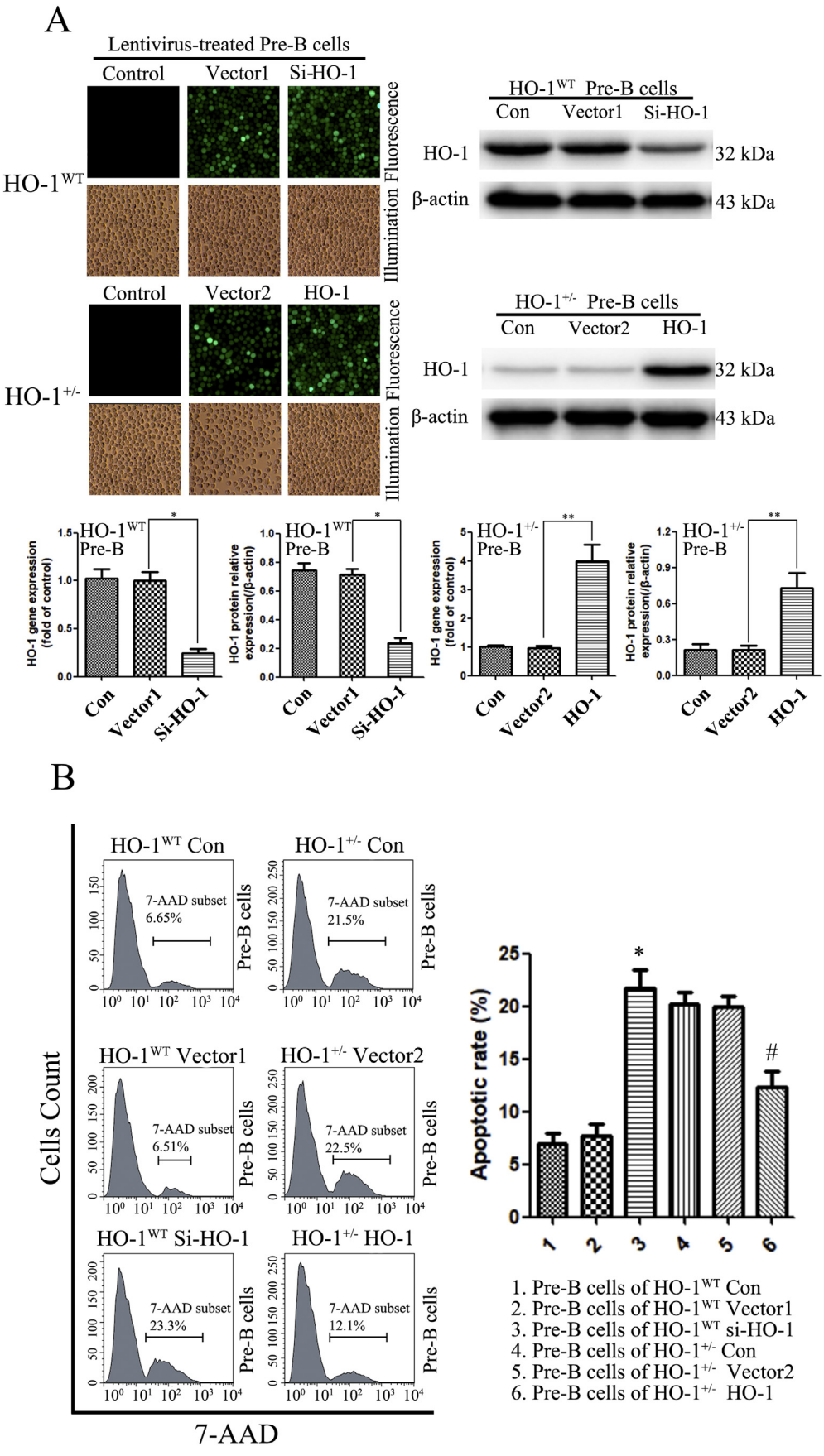

Fig. 7. Effects of HO-1 protein on Pre-B cell apoptosis.

(A) Pre-B cells were isolated from bone marrow cells of HO-1^{WT} and HO-1$^{+/-}$ mice by FACS. Next, lentivirus-mediated HO-1 gene overexpression in Pre-B cells of HO-1$^{+/-}$ mice and HO-1 gene silencing in Pre-B cells of HO-1^{WT} mice, as well as positivity of lentivirus-mediated HO-1 transduction (> 95%) were observed by fluorescence microscopy. HO-1 gene and protein expressions were detected by real-time PCR and Western blot, respectively. (B) After treatment with lentivirus for 48 h, cells cycle arrest was detected by FCM. *Comparison between control and siHO-1 in HO-1^{WT} mice, $P < 0.05$. #Comparison between control and siHO-1 in HO-1$^{+/-}$ mice, $P < 0.01$. Data were analyzed with GraphPad Prism V5.0 software.

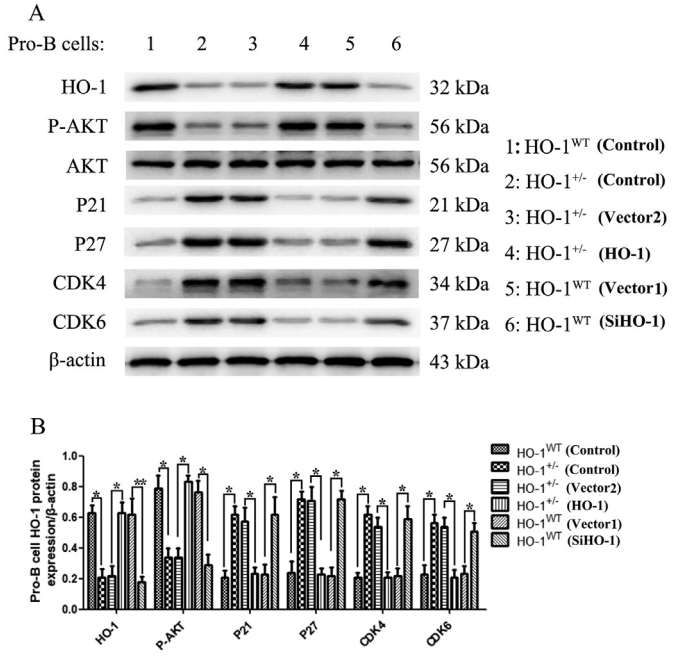

Fig. 8. The PI3K/AKT pathway was involved in Pro-B cell cycle arrest.
(A and B) Lentivirus-mediated HO-1 gene up-regulation in Pro-B cells of HO-$1^{+/-}$ mice and HO-1 gene silencing in Pro-B cells of HO-1^{WT} mice. The expressions of HO-1, P-AKT, AKT, P21, P27, CDK4 and CDK6 proteins were detected by Western blot. Western blot bands were quantified with Quantity One software. Each sample was normalized by relative β-actin expression. All experiments were repeated three times. *P < 0.05, **P < 0.01.

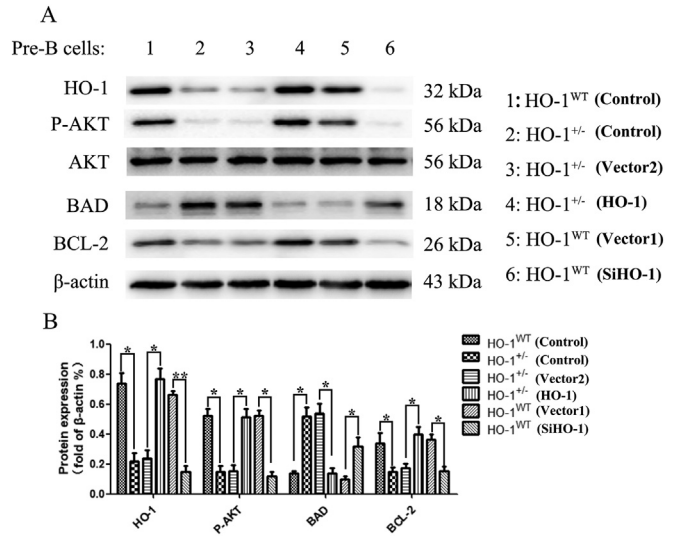

Fig. 9. The PI3K/AKT pathway was involved in Pre-B cell apoptosis.
(A and B) Lentivirus-mediated HO-1 gene up-regulation in Pre-B cells of HO-$1^{+/-}$ mice and HO-1 gene silencing in Pre-B cells of HO-1^{WT} mice. The expressions of HO-1, P-AKT, AKT, BAD and BCL-2 proteins were detected by Western blot. Western blot bands were quantified with Quantity One software. Each sample was normalized by relative β-actin expression. All experiments were repeated three times. *P < 0.05, **P < 0.01.

studied the development of B cells in the spleen, and confirmed that the absolute numbers of all B cell subtypes in HO-$1^{+/-}$ mice were significantly lower than those of HO-1^{WT} mice, suggesting that the absence of HO-1 decreased the absolute counts of various B cell subsets and blocked B cell maturation in the spleen.

In bone marrow, lymphoid-primed multipotent progenitors commit to the lymphoid branch by generating common lymphoid progenitors, which, in turn, generate early B and T lymphocyte progenitors [2]. Herein, there were significantly fewer Pre-B cells as well as mature and recirculating B cells in the bone marrow of HO-$1^{+/-}$ mice than those of HO-1^{WT} mice. Contrarily, HO-$1^{+/-}$ mice had more Pro-B cells. In addition, HO-1 deficiency caused Pro-B cells to undergo a series of differentiation steps during the abnormal generation of Pre-B cells, which blocked B cell development at the Pro-B to Pre-B cell transition. Notably, Pre-B cells lacking HO-1 were more susceptible to apoptosis than HO-1^{WT} ones. Altogether, Pro-B cells failed to differentiate into Pre-B cells owing to the lack of HO-1, which may be responsible for the sharply reduced numbers of pre-B and subsequent B cell subsets in the bone marrow and PB of HO-1 deficient mice. In short, we verified, for the first time, that HO-1 was necessary for early B cell development.

Since this study used HO-$1^{+/-}$ mice instead of HO-$1^{-/-}$ mice, there were limitations such as poor targeting ability. HO-1 gene was knocked out from mice with a conventional method, so HO-$1^{-/-}$ mice died in the embryonic period. Similarly, Travis et al. reported that HO-1 was involved in the differentiation of immune cells in bone marrow upon renal ischemia-reperfusion injury, and HO-1 deficient mice had myeloid-specific HO-1 deficiency [43]. By conditionally deleting HO-1 in hepatocytes and macrophages, Alexander et al. found that mice managed to combat diet-induced insulin resistance and inflammation. Particularly, HO-1 deficiency in other tissues barely affected the differentiation of bone marrow cells [33].

Furthermore, *in vitro* experiments were conducted by up-regulating HO-1 in the Pro-B cells of HO-$1^{+/-}$ mice and silencing it in the cells of HO-1^{WT} mice through lentiviral transduction. The down-regulation of HO-1 expression significantly promoted the G0/G1 phase arrest of Pro-B cells *in vitro*. In addition, HO-1 up-regulation significantly inhibited Pre-B cell apoptosis *in vitro*. The PI3K/AKT signaling pathway was possibly involved in the regulation of early B lymphocyte development induced by HO-1 deficiency. Strikingly, the absence of HO-1 from Pro-B cells was associated with activation of the PI3K/AKT pathway, leading to up-regulated expressions of key proteins for cell cycle arrest, such as P21, P27, CDK4 and CDK6. Although increasing HO-1 protein expression augmented the expression of P-AKT protein, AKT protein expression was not significantly affected. The phosphorylation of AKT protein is usually linked to its activity, and HO-1 promoted expression of P-AKT protein can activate the PI3K/AKT pathway. In this study, nevertheless, the expression of P-AKT also reduced after HO-1 protein expression in the Pre-B cells of HO-1^{WT} mice was down-regulated. When the PI3K/AKT pathway was suppressed, the inhibited expressions of downstream apoptosis proteins, such as BAD and BCL-2, were weakened. Accordingly, HO-1 was required for AKT-mediated inhibition of apoptosis and cell cycle arrest. Cudmore et al. also found P-AKT reduction in the organs of HO-1 null mice, and identified an inter-dependency between AKT and HO-1 [46]. In-depth studies using gene microarray, co-immunoprecipitation assay and chromatin immunoprecipitation assay to reveal the interactions between HO-1 and key factors in micro-environment are ongoing in our group.

5. Conclusions

In conclusion, HO-1 was a key factor regulating the proliferation and development of B cells in mice. Our findings pave the way for unraveling the transcriptional complexity underlying B cell generation.

Author contributions

Jishi Wang, Dan Ma and Zhen Zhou conceived and designed the study. Peifan Li, Danna Wei, Ping Liu, Kunling Yu, Ping Wang and Qin Fang performed research.

Dan Ma and Zhen Zhou contribute equally to this study.

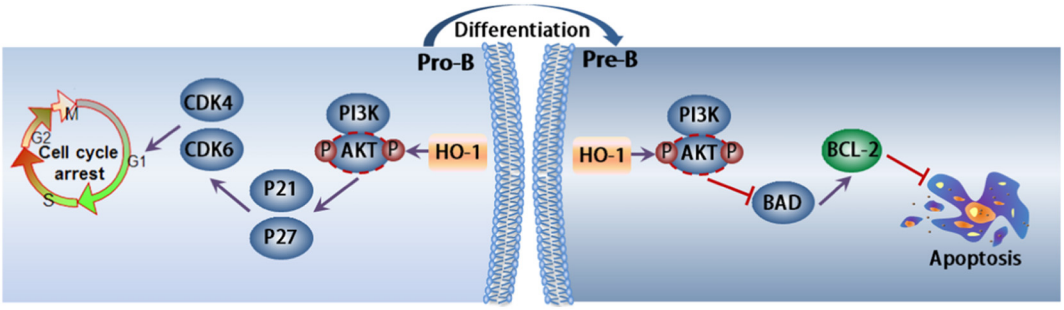

Fig. 10. Schematic representation of mechanism for influence of HO-1 protein on B cell development.
The schematic representation of mechanism for the relationship of HO-1 with the PI3K/AKT pathway and its downstream proteins.

Funding

This study was supported, in part, by the National Natural Science Foundation of China (No. 81070444, 81270636, 81360501, 81470006, 81660616 and 81760670); Guizhou province Technology Bureau Union Fund (No. Union LH-2015-7386); Doctor-special Scientific Research Foundation of Guizhou Medical University (I-2017-20); Guiyang Health Fund Zhu kehetong [2018, 1-74].

Statement of ethics

In the animal experiments, all procedures were conducted in accordance with Guidelines for the Care and Use of Laboratory Animals. The protocol was approved by the Committee on the Ethics of Animal Experiments of Guiyang Medical University (No. 1603133).

Declaration of Competing Interest

The authors declare no conflict of interest.

Acknowledgement

First and foremost, I would like to show my deepest gratitude to my supervisor, Dr. Jishi Wang, a respectable, responsible and resourceful scholar, who has provided me with valuable guidance in every stage of the writing of this thesis.

Appendix A. Supplementary data

Supplementary data to this article can be found online at https://doi.org/10.1016/j.cellsig.2019.109378.

References

[1] W. Qiao, W. Wang, E. Laurenti, A.L. Turinsky, S.J. Wodak, G.D. Bader, J.E. Dick, P.W. Zandstra, Intercellular network structure and regulatory motifs in the human hematopoietic system, Mol. Syst. Biol. 10 (2014) 741.
[2] A. Azagra, L. Roman-Gonzalez, O. Collazo, J. Rodriguez-Ubreva, V.G. de Yebenes, B. Barneda-Zahonero, J. Rodriguez, M. Castro de Moura, J. Grego-Bessa, I. Fernandez-Duran, A.B. Islam, M. Esteller, A.R. Ramiro, E. Ballestar, M. Parra, In vivo conditional deletion of HDAC7 reveals its requirement to establish proper B lymphocyte identity and development, J. Exp. Med. 213 (12) (2016) 2591–2601.
[3] E. Montecino-Rodriguez, K. Dorshkind, B-1 B cell development in the fetus and adult, Immunity 36 (1) (2012) 13–21.
[4] K. Pieper, B. Grimbacher, H. Eibel, B-cell biology and development, J. Allergy Clin. Immunol. 131 (4) (2013) 959–971.
[5] T. Muliaditan, J. Caron, M. Okesola, J.W. Opzoomer, P. Kosti, M. Georgouli, P. Gordon, S. Lall, D.M. Kuzeva, L. Pedro, J.D. Shields, C.E. Gillett, S.S. Diebold, V. Sanz-Moreno, T. Ng, E. Hoste, J.N. Arnold, Macrophages are exploited from an innate wound healing response to facilitate cancer metastasis, Nat. Commun. 9 (1) (2018) 2951.
[6] L. Jia, Y. Wang, Y. Wang, Y. Ma, J. Shen, Z. Fu, Y. Wu, S. Su, Y. Zhang, Z. Cai, J. Wang, M. Xiang, Heme oxygenase-1 in macrophages drives septic cardiac dysfunction via suppressing lysosomal degradation of inducible nitric oxide synthase, Circ. Res. 122 (11) (2018) 1532–1544.
[7] R. Gozzelino, V. Jeney, M.P. Soares, Mechanisms of cell protection by heme oxygenase-1, Annu. Rev. Pharmacol. Toxicol. 50 (2010) 323–354.
[8] G. Li Volti, D. Tibullo, L. Vanella, C. Giallongo, F. Di Raimondo, S. Forte, M. Di Rosa, S.S. Signorelli, I. Barbagallo, The Heme oxygenase system in Hematological malignancies, Antioxid. Redox Signal. 27 (6) (2017) 363–377.
[9] L.Y. Chau, Heme oxygenase-1: emerging target of cancer therapy, J. Biomed. Sci. 22 (2015) 22.
[10] P. Liu, D. Ma, Z. Yu, N. Zhe, M. Ren, P. Wang, M. Yu, J. Huang, Q. Fang, J. Wang, Overexpression of heme oxygenase-1 in bone marrow stromal cells promotes microenvironment-mediated imatinib resistance in chronic myeloid leukemia, Biomed. Pharmacother. 91 (2017) 21–30.
[11] M.K. Herroon, E. Rajagurubandara, J.D. Diedrich, E.I. Heath, I. Podgorski, Adipocyte-activated oxidative and ER stress pathways promote tumor survival in bone via upregulation of Heme oxygenase 1 and Survivin, Sci. Rep. 8 (1) (2018) 40.
[12] M. Kozakowska, K. Szade, J. Dulak, A. Jozkowicz, Role of heme oxygenase-1 in postnatal differentiation of stem cells: a possible cross-talk with microRNAs, Antioxid. Redox Signal. 20 (11) (2014) 1827–1850.
[13] H.B. Suliman, F. Zobi, C.A. Piantadosi, Heme Oxygenase-1/carbon monoxide system and embryonic stem cell differentiation and maturation into cardiomyocytes, Antioxid. Redox Signal. 24 (7) (2016) 345–360.
[14] K.D. Poss, S. Tonegawa, Heme oxygenase 1 is required for mammalian iron reutilization, Proc. Natl. Acad. Sci. U. S. A. 94 (20) (1997) 10919–10924.
[15] K.D. Poss, S. Tonegawa, Reduced stress defense in heme oxygenase 1-deficient cells, Proc. Natl. Acad. Sci. U. S. A. 94 (20) (1997) 10925–10930.
[16] A. Jais, E. Einwallner, O. Sharif, K. Gossens, T. Lu, S.M. Soyal, D. Medgyesi, D. Neureiter, J. Paier-Pourani, K. Dalgaard, J.C. Duvigneau, J. Lindroos-Christensen, T.C. Zapf, S. Amann, S. Saluzzo, F. Jantscher, P. Stiedl, J. Todoric, R. Martins, H. Oberkofler, S. Muller, C. Hauser-Kronberger, L. Kenner, E. Casanova, H. Sutterluty-Fall, M. Bilban, K. Miller, A.V. Kozlov, F. Krempler, S. Knapp, C.N. Lumeng, W. Patsch, O. Wagner, J.A. Pospisilik, H. Esterbauer, Heme oxygenase-1 drives metaflammation and insulin resistance in mouse and man, Cell 158 (1) (2014) 25–40.
[17] L.F. Wang, K.K. Yokoyama, C.L. Lin, T.Y. Chen, H.W. Hsiao, P.C. Chiang, C. Hsu, Knockout of ho-1 protects the striatum from ferrous iron-induced injury in a male-specific manner in mice, Sci. Rep. 6 (2016) 26358.
[18] X. Lin, Q. Fang, S. Chen, N. Zhe, Q. Chai, M. Yu, Y. Zhang, Z. Wang, J. Wang, Heme oxygenase-1 suppresses the apoptosis of acute myeloid leukemia cells via the JNK/c-JUN signaling pathway, Leuk. Res. 39 (5) (2015) 544–552.
[19] V. Kapoor, A. Khudanyan, P. de la Puente, J. Campian, D.E. Hallahan, A.K. Azab, D. Thotala, Stem cell transfusion restores immune function in radiation-induced Lymphopenic C57BL/6 mice, Cancer Res. 75 (17) (2015) 3442–3445.
[20] C.L. Lee, K.D. Castle, E.J. Moding, J.M. Blum, N. Williams, L. Luo, Y. Ma, L.B. Borst, Y. Kim, D.G. Kirsch, Acute DNA damage activates the tumour suppressor p53 to promote radiation-induced lymphoma, Nat. Commun. 6 (2015) 8477.
[21] Z. Gong, H. Xu, Y. Su, W. Wu, L. Hao, C. Han, Establishment of a novel bladder cancer xenograft model in humanized immunodeficient mice, Cell. Physiol. Biochem. 37 (4) (2015) 1355–1368.
[22] X. An, L. Chen, Flow cytometry (FCM) analysis and fluorescence-activated cell sorting (FACS) of erythroid cells, Methods Mol. Biol. 1698 (2018) 153–174.
[23] K. de Wijs, C. Liu, A. Dusa, D. Vercruysse, B. Majeed, D.S. Tezcan, K. Blaszkiewicz, J. Loo, L. Lagae, Micro vapor bubble jet flow for safe and high-rate fluorescence-activated cell sorting, Lab Chip 17 (7) (2017) 1287–1296.
[24] L. Liu, T.H. Cheung, G.W. Charville, T.A. Rando, Isolation of skeletal muscle stem cells by fluorescence-activated cell sorting, Nat. Protoc. 10 (10) (2015) 1612–1624.
[25] S. Shojaee, L.N. Chan, M. Buchner, V. Cazzaniga, K.N. Cosgun, H. Geng, Y.H. Qiu, M.D. von Minden, T. Ernst, A. Hochhaus, G. Cazzaniga, A. Melnick, S.M. Kornblau, T.G. Graeber, H. Wu, H. Jumaa, M. Muschen, PTEN opposes negative selection and enables oncogenic transformation of pre-B cells, Nat. Med. 22 (4) (2016) 379–387.
[26] I. Joshi, T. Yoshida, N. Jena, X. Qi, J. Zhang, R.A. Van Etten, K. Georgopoulos, Loss of Ikaros DNA-binding function confers integrin-dependent survival on pre-B cells and progression to acute lymphoblastic leukemia, Nat. Immunol. 15 (3) (2014) 294–304.
[27] S.H. Pang, M. Minnich, P. Gangatirkar, Z. Zheng, A. Ebert, G. Song, R.A. Dickins, L.M. Corcoran, C.G. Mullighan, M. Busslinger, N.D. Huntington, S.L. Nutt, S. Carotta, PU.1 cooperates with IRF4 and IRF8 to suppress pre-B-cell leukemia, Leukemia 30 (6) (2016) 1375–1387.
[28] K. Zambrano, V. Jerome, R. Freitag, R. Buchholz, H.M. Jack, H. Hubner, W. Schuh, Prolonged ex vivo expansion and differentiation of naive murine CD43(−) B

splenocytes, Biotechnol. Prog. 32 (4) (2016) 978–989.
[29] L. Han, J. Jiang, Q. Ma, Z. Wu, Z. Wang, The inhibition of heme oxygenase-1 enhances the chemosensitivity and suppresses the proliferation of pancreatic cancer cells through the SHH signaling pathway, Int. J. Oncol. 52 (6) (2018) 2101–2109.
[30] J. Huang, P. Guo, D. Ma, X. Lin, Q. Fang, J. Wang, Overexpression of heme oxygenase-1 induced by constitutively activated NF-kappaB as a potential therapeutic target for activated B-cell-like diffuse large B-cell lymphoma, Int. J. Oncol. 49 (1) (2016) 253–264.
[31] D. Ma, Q. Fang, P. Wang, R. Gao, W. Wu, T. Lu, L. Cao, X. Hu, J. Wang, Induction of heme oxygenase-1 by Na+-H+ exchanger 1 protein plays a crucial role in imatinib-resistant chronic myeloid leukemia cells, J. Biol. Chem. 290 (20) (2015) 12558–12571.
[32] D. Ma, Q. Fang, P. Wang, R. Gao, J. Sun, Y. Li, X.Y. Hu, J.S. Wang, Downregulation of HO-1 promoted apoptosis induced by decitabine via increasing p15INK4B promoter demethylation in myelodysplastic syndrome, Gene Ther. 22 (4) (2015) 287–296.
[33] P. Wang, D. Ma, J. Wang, Q. Fang, R. Gao, W. Wu, T. Lu, L. Cao, Silencing HO-1 sensitizes SKM-1 cells to apoptosis induced by low concentration 5-azacytidine through enhancing p16 demethylation, Int. J. Oncol. 46 (3) (2015) 1317–1327.
[34] G. Kano, M. Almanan, B.S. Bochner, N. Zimmermann, Mechanism of Siglec-8-mediated cell death in IL-5-activated eosinophils: role for reactive oxygen species-enhanced MEK/ERK activation, J. Allergy Clin. Immunol. 132 (2) (2013) 437–445.
[35] S. Melzer, C.S. Nunes, D.C. Endringer, T.U. de Andrade, A. Tarnok, D. Lenz, Trypan blue as an affordable marker for automated live-dead cell analysis in image cytometry, Scanning 38 (6) (2016) 857–863.
[36] S. Tang, B. Cheng, N. Zhe, D. Ma, J. Xu, X. Li, Y. Guo, W. Wu, J. Wang, Histone deacetylase inhibitor BG45-mediated HO-1 expression induces apoptosis of multiple myeloma cells by the JAK2/STAT3 pathway, Anti-Cancer Drugs 29 (1) (2018) 61–74.
[37] Z. Zhou, Q. Fang, D. Ma, N. Zhe, M. Ren, B. Cheng, P. Li, P. Liu, X. Lin, S. Tang, X. Hu, Y. Liao, Y. Zhang, T. Lu, J. Wang, Silencing heme oxygenase-1 increases the sensitivity of ABC-DLBCL cells to histone deacetylase inhibitor in vitro and in vivo, Oncotarget 8 (45) (2017) 78480–78495.
[38] A. Abdelbaset-Ismail, S. Borkowska-Rzeszotek, E. Kubis, K. Bujko, K. Brzezniakiewicz-Janus, L. Bolkun, J. Kloczko, M. Moniuszko, G.W. Basak, W. Wiktor-Jedrzejczak, M.Z. Ratajczak, Activation of the complement cascade enhances motility of leukemic cells by downregulating expression of HO-1, Leukemia 31 (2) (2017) 446–458.
[39] P. Banerjee, A. Basu, B. Wegiel, L.E. Otterbein, K. Mizumura, M. Gasser, A.M. Waaga-Gasser, A.M. Choi, S. Pal, Heme oxygenase-1 promotes survival of renal cancer cells through modulation of apoptosis- and autophagy-regulating molecules, J. Biol. Chem. 287 (38) (2012) 32113–32123.
[40] M.D. Hjortso, M.H. Andersen, The expression, function and targeting of haem oxygenase-1 in cancer, Curr. Cancer Drug Targets 14 (4) (2014) 337–347.
[41] L. Cao, J. Wang, D. Ma, P. Wang, Y. Zhang, Q. Fang, Heme oxygenase-1 contributes to imatinib resistance by promoting autophagy in chronic myeloid leukemia through disrupting the mTOR signaling pathway, Biomed. Pharmacother. 78 (2016) 30–38.
[42] W. Wu, D. Ma, P. Wang, L. Cao, T. Lu, Q. Fang, J. Zhao, J. Wang, Potential crosstalk of the interleukin-6-heme oxygenase-1-dependent mechanism involved in resistance to lenalidomide in multiple myeloma cells, FEBS J. 283 (5) (2016) 834–849.
[43] S. Wei, Y. Wang, Q. Chai, Q. Fang, Y. Zhang, J. Wang, Potential crosstalk of Ca2+-ROS-dependent mechanism involved in apoptosis of Kasumi-1 cells mediated by heme oxygenase-1 small interfering RNA, Int. J. Oncol. 45 (6) (2014) 2373–2384.
[44] S. Tang, D. Ma, B. Cheng, Q. Fang, X. Kuang, K. Yu, W. Wang, B. Hu, J. Wang, Crucial role of HO-1/IRF4-dependent apoptosis induced by panobinostat and lenalidomide in multiple myeloma, Exp. Cell Res. 363 (2) (2018) 196–207 Feb 15.
[45] N. Zhe, J. Wang, S. Chen, X. Lin, Q. Chai, Y. Zhang, J. Zhao, Q. Fang, Heme oxygenase-1 plays a crucial role in chemoresistance in acute myeloid leukemia, Hematology 20 (7) (2015) 384–391.
[46] M.J. Cudmore, S. Ahmad, S. Sissaoui, W. Ramma, B. Ma, T. Fujisawa, B. Al-Ani, K. Wang, M. Cai, F. Crispi, P.W. Hewett, E. Gratacos, S. Egginton, A. Ahmed, Loss of Akt activity increases circulating soluble endoglin release in preeclampsia: identification of inter-dependency between Akt-1 and heme oxygenase-1, Eur. Heart J. 33 (9) (2012) 1150–1158.